Cell, Vol. 122, 669–682, September 9, 2005, Copyright ©2005 by Elsevier Inc. DOI 10.1016/j.cell.2005.08.012

Identification and Characterization of MAVS, a Mitochondrial Antiviral Signaling Protein that Activates NF-κB and IRF3

Rashu B. Seth,[1] Lijun Sun,[1] Chee-Kwee Ea, and Zhijian J. Chen*
Howard Hughes Medical Institute
Department of Molecular Biology
University of Texas Southwestern Medical Center
Dallas, Texas 75390

Summary

Viral infection triggers host innate immune responses through activation of the transcription factors NF-κB and IRF3, which coordinately regulate the expression of type-I interferons such as interferon-β (IFN-β). Herein, we report the identification of a novel protein termed MAVS (*m*itochondrial *a*nti*v*iral *s*ignaling), which mediates the activation of NF-κB and IRF3 in response to viral infection. Silencing of MAVS expression through RNA interference abolishes the activation of NF-κB and IRF3 by viruses, thereby permitting viral replication. Conversely, overexpression of MAVS induces the expression of IFN-β through activation of NF-κB and IRF3, thus boosting antiviral immunity. Epistasis experiments show that MAVS is required for the phosphorylation of IRF3 and IκB and functions downstream of RIG-I, an intracellular receptor for viral RNA. MAVS contains an N-terminal CARD-like domain and a C-terminal transmembrane domain, both of which are essential for MAVS signaling. The transmembrane domain targets MAVS to the mitochondria, implicating a new role of mitochondria in innate immunity.

Introduction

Viral infection of host cells triggers innate and adaptive immune responses that are essential for the survival of the host. A highly effective antiviral immune response is the production of type-I interferons, such as interferon-α (IFN-α) and interferon-β (IFN-β). These interferons activate the JAK-STAT pathway to stimulate the expression of interferon-stimulated genes (ISGs), which collectively inhibit viral replication and assembly (Darnell et al., 1994). The genes encoding interferons are regulated by the assembly of an enhanceosome containing several transcription factors including NF-κB and IRF3, both of which are regulated by subcellular localization (Maniatis et al., 1998). In unstimulated cells, NF-κB is sequestered in the cytoplasm in association with an inhibitor of the IκB family (Baeuerle and Baltimore, 1988). Stimulation of cells with cytokines (e.g., TNFα or IL-1β) or pathogens (e.g., bacteria or viruses) leads to the activation of a large kinase complex consisting of the catalytic subunits IKKα and IKKβ and the essential regulatory subunit NEMO (also known as IKKγ or IKKAP). The activated IKK complex phosphorylates IκB and targets this inhibitor for degradation by the ubiquitin-proteasome pathway. NF-κB is then liberated to enter the nucleus to turn on a battery of genes essential for immune and inflammatory responses (Silverman and Maniatis, 2001).

Similar to NF-κB, IRF3 is also retained in the cytoplasm of unstimulated cells. After viral or bacterial infection of cells, IRF3 is phosphorylated at multiple serine and threonine residues at the C terminus (Hiscott et al., 2003; Yoneyama et al., 2002). The phosphorylated IRF3 then homodimerizes and enters the nucleus to activate IFN-β in a highly cooperative manner with NF-κB. The kinases that phosphorylate IRF3 have recently been identified as the IKK-like kinases TBK1 and IKKε (Fitzgerald et al., 2003; Sharma et al., 2003). Genetic experiments have shown that TBK1 is important for interferon production by the bacterial cell wall component lipopolysaccharides (LPS) as well as viruses (Hemmi et al., 2004; McWhirter et al., 2004). In some cells, however, the function of TBK1 may be compensated by IKKε or other kinases (Perry et al., 2004; Yoneyama et al., 2004). TBK1 and IKKε can also phosphorylate and activate IRF7 (tenOever et al., 2004), another IRF family member essential for the production of type-I interferons such as interferon-α (Honda et al., 2005).

Both NF-κB and IRFs are tightly regulated by microbial pathogens, including RNA viruses. After entry into host cell and uncoating of an RNA virus, the viral RNA replicates to produce double-stranded RNA intermediates, which are recognized by the host as a pathogen-associated molecular pattern (PAMP). Several proteins that recognize viral RNA have been discovered, including Toll-like receptors TLR3, 7, and 8 (Akira and Takeda, 2004). TLR3 contains an intracellular Toll-interleukin receptor (TIR) domain that signals to NF-κB and IRF3 via the adaptor protein TRIF (Akira and Takeda, 2004), whereas the TIR domain of TLR7 and TLR8 binds to another adaptor MyD88, which associates with and activates IRF7 to induce interferon-α (Kawai et al., 2004). In addition, TLRs contain several extracellular leucine-rich repeats (LRRs) that presumably recognize microbial ligands. Thus, the topology of these receptors dictates that they can only recognize extracellular dsRNA or single-stranded RNA associated with viral particles that are internalized into the endosomes (Crozat and Beutler, 2004). The receptor that detects intracellular dsRNA generated by the virus is a newly identified protein RIG-I, which contains two N-terminal CARD-like domains, and a C-terminal RNA helicase domain that binds to dsRNA (Sumpter et al., 2005; Yoneyama et al., 2004). Presumably, the binding of viral RNA to RIG-I leads to a conformational change that exposes the CARD-like domain, which then activates downstream signaling. Consistent with this model, overexpression of the N-terminal CARD-like domains of RIG-I is sufficient to activate both NF-κB and IRF3 (Yoneyama et al., 2004). However, the mechanism by which RIG-I activates NF-κB and IRF3 is currently not understood. A RIG-I-like protein MDA-5 (also known as HELICARD),

*Correspondence: zhijian.chen@utsouthwestern.edu
[1]These authors contributed equally to this work.

which also contains two CARD-like domains and an RNA helicase domain, has recently been shown to be involved in dsRNA signaling and apoptosis (Andrejeva et al., 2004; Kang et al., 2002; Kovacsovics et al., 2002). However, MDA-5 does not appear to function redundantly with RIG-I in the antiviral pathway, as an inactivating mutation of RIG-I or the loss of RIG-I expression completely blocks interferon production by several RNA viruses (Kato et al., 2005; Sumpter et al., 2005; Yoneyama et al., 2004).

Here, we report the identification of a novel protein that is essential for NF-κB and IRF3 activation by RNA viruses. This protein, named MAVS (mitochondrial antiviral signaling), contains an N-terminal CARD-like domain and a C-terminal transmembrane domain that targets the protein to the mitochondrial membrane. MAVS functions downstream of RIG-I and upstream of IκB and IRF3 phosphorylation. Suppression of MAVS expression blocked interferon production and exacerbated the viral replication and killing of the host cells. Conversely, overexpression of MAVS augmented interferon production and conferred antiviral immunity. Deletion of the CARD-like domain of MAVS abolished its signaling function and converted it into a dominant-negative mutant that inhibited interferon induction. Importantly, the mitochondrial targeting transmembrane domain is also essential for MAVS signaling, thus implicating a new role of mitochondria in innate immunity.

Results

Identification and Sequence Analysis of MAVS

To understand the signaling pathways required for the activation of NF-κB and IRF3 by viruses, we sought to identify proteins containing CARD-like domains similar to those of RIG-I and its homolog MDA-5. A BLAST search with the first CARD-like domain of MDA-5 identified an uncharacterized protein KIAA1271, which contains a single CARD-like domain at the N terminus. Interestingly, this protein was also identified as a putative NF-κB activator in a large-scale screening for proteins that can activate an NF-κB reporter when they are overexpressed (Matsuda et al., 2003). However, there was no further characterization of this protein concerning its domain structure, activity, or biological function. We have analyzed the sequence of this protein, and found that in addition to the N-terminal CARD-like domain, which is conserved from pufferfish to human (Figures 1A–1C), KIAA1271 also contains a proline-rich region in the middle and a hydrophobic transmembrane domain at the C terminus (Figure 1D). The transmembrane domain was predicted using two different programs: TMpred (http://www.ch.embnet.org/software/TMPRED_form.html; Figure 1D), and Kyte-Doolittle hydropathy plot (data not shown). As will be shown later (Figure 7), this transmembrane domain targets KIAA1271 to the mitochondria. We therefore designated this protein as mitochondrial antiviral signaling (MAVS) protein.

MAVS Activates NF-κB, IRF3, and IRF7 to Induce Interferons

Although overexpression of many proteins can activate NF-κB, a much smaller number of proteins can activate both NF-κB and IRF3, which are required for the induction of interferons. We therefore tested whether MAVS could activate a luciferase reporter that is under the control of the IFN-β promoter. This promoter contains enhancer elements that bind to several transcription factors including NF-κB, IRF3, and ATF2. The coordinate activation of all of these transcription factors is required for the formation of an enhanceosome that activates IFN-β. Significantly, overexpression of MAVS in HEK293 cells potently activates the IFN-β promoter (Figure 2A). In control experiments, infection of the same cells with the Sendai virus (S.V.), an RNA virus of the paramyxoviridae family, leads to the activation of IFN-β. Similarly, overexpression of the tandem N-terminal CARD-like domains of RIG-I (designated as RIG-I(N)) also induces IFN-β. In contrast, overexpression of another CARD domain protein RIP2 (Inohara et al., 1998), which is known to activate NF-κB but not IRF3 in response to intracellular bacterial infection, failed to induce IFN-β. Consistent with the ability of MAVS to induce the assembly of the IFN-β enhanceosome, MAVS activated both IRF3 (Figure 2B) and NF-κB (Figure 2C). In the former case, the activation of IRF3 was measured by the phosphorylation and dimerization of a chimeric protein consisting of IRF3 fused to the DNA binding domain of Gal4, which drives the expression of the luciferase reporter gene. In the latter case, NF-κB activation was measured using a luciferase reporter whose expression was driven by three copies of an NF-κB enhancer. We also examined whether MAVS activates JNK, which is known to phosphorylate and activate ATF2. Similar to RIP2, overexpression of MAVS led to the activation of JNK, as measured by immunoblotting with an antibody specific for phosphorylated JNK (see Figure S1A in the Supplemental Data available with this article online). Overexpression of MAVS also induced the production of endogenous IFN-β, as determined by ELISA of culture supernatants (Figure 2D). RT-PCR experiments showed that MAVS induced IFN-β and the chemokine RANTES, but not the housekeeping gene GAPDH, at the RNA level (Figure 2E). Immunoblotting experiments showed that MAVS activated IRF3 by inducing the phosphorylation (Figure 2F, upper panel) and dimerization of IRF3 (Figure 2F, lower panel). To determine if MAVS also activates IRF7, a master regulator of IFN-α, we cotransfected MAVS, IRF7, and an IFN-α luciferase reporter into HEK293 cells, which do not express endogenous IRF7. Similar to Sendai virus infection, overexpression of MAVS or RIG-I(N) potently induced IFN-α promoter activity (Figure S1B). Collectively, these results show that MAVS is a potent activator of IRF3, IRF7, and NF-κB and that its overexpression is sufficient to mimic viral infection to induce cytokines including IFN-α, IFN-β, and RANTES.

MAVS Is Required for IKK and IRF3 Activation and IFN-β Induction by Sendai Virus

To determine if MAVS is required for IFN-β induction by viruses, we used RNAi to silence the expression of endogenous MAVS, which was detected with an affinity-purified MAVS antibody against a fragment of MAVS containing amino acids 131–291. This antibody detected multiple bands in whole-cell lysates derived

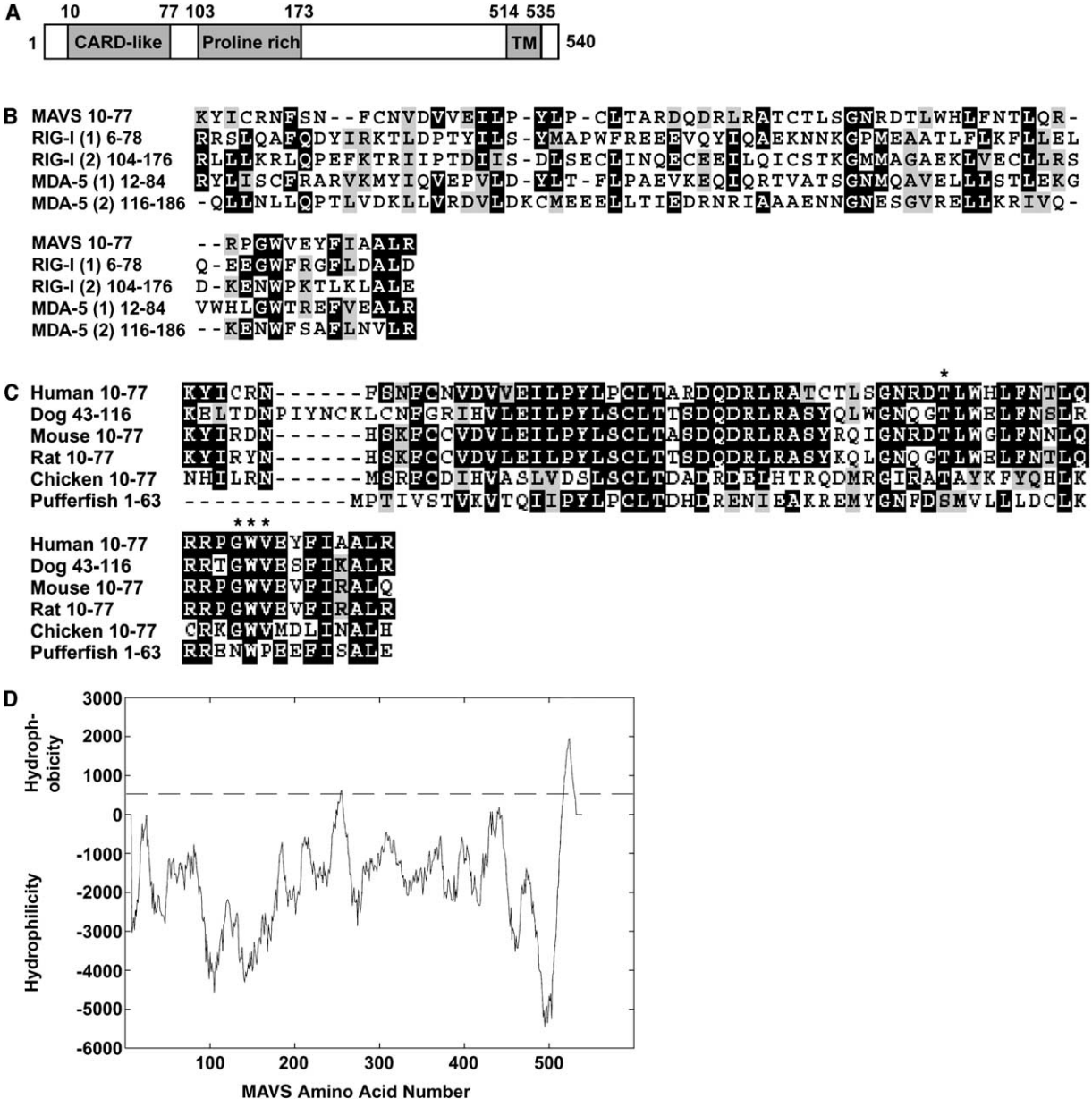

Figure 1. Domain and Sequence Analyses of MAVS

(A) A schematic diagram of MAVS protein. TM: transmembrane domain.

(B) Sequence alignment of the CARD-like domains of MAVS, RIG-I and MDA-5, using the Clustal W program.

(C) Sequence alignment of the CARD-like domains of MAVS from different species based on the genome projects. The asterisk (*) indicates the residues that were mutated to alanine in Figure 6A.

(D) Prediction of the MAVS transmembrane domain using the TMpred server. A score of greater than 500 predicts a transmembrane region.

from HEK293 cells as well as those transfected with the control GFP siRNA oligos (Figure 3A, lower panel). These bands disappeared in cells transfected with two different pairs of siRNA oligos targeting distinct regions of MAVS, indicating that the bands detected by the antibody were indeed MAVS proteins. It is not clear why MAVS protein exists as multiple bands on SDS-PAGE, but it is unlikely that they represent different spliced variants, as the same expression pattern was observed when cells were transfected with MAVS cDNA (data not shown). The pattern of these bands did not change when cell extracts were treated with phosphatases or glycosidase (data not shown), suggesting that they are not the phosphorylated or glycosylated forms of MAVS. We have also been unable to obtain evidence of MAVS modification by ubiquitin or ubiquitin-like proteins such as ISG-15. Thus, it is likely that the lower bands represent the degradation or processing products of MAVS, whereas the upper band is the full-length MAVS protein. The MAVS protein bands were detected by immu-

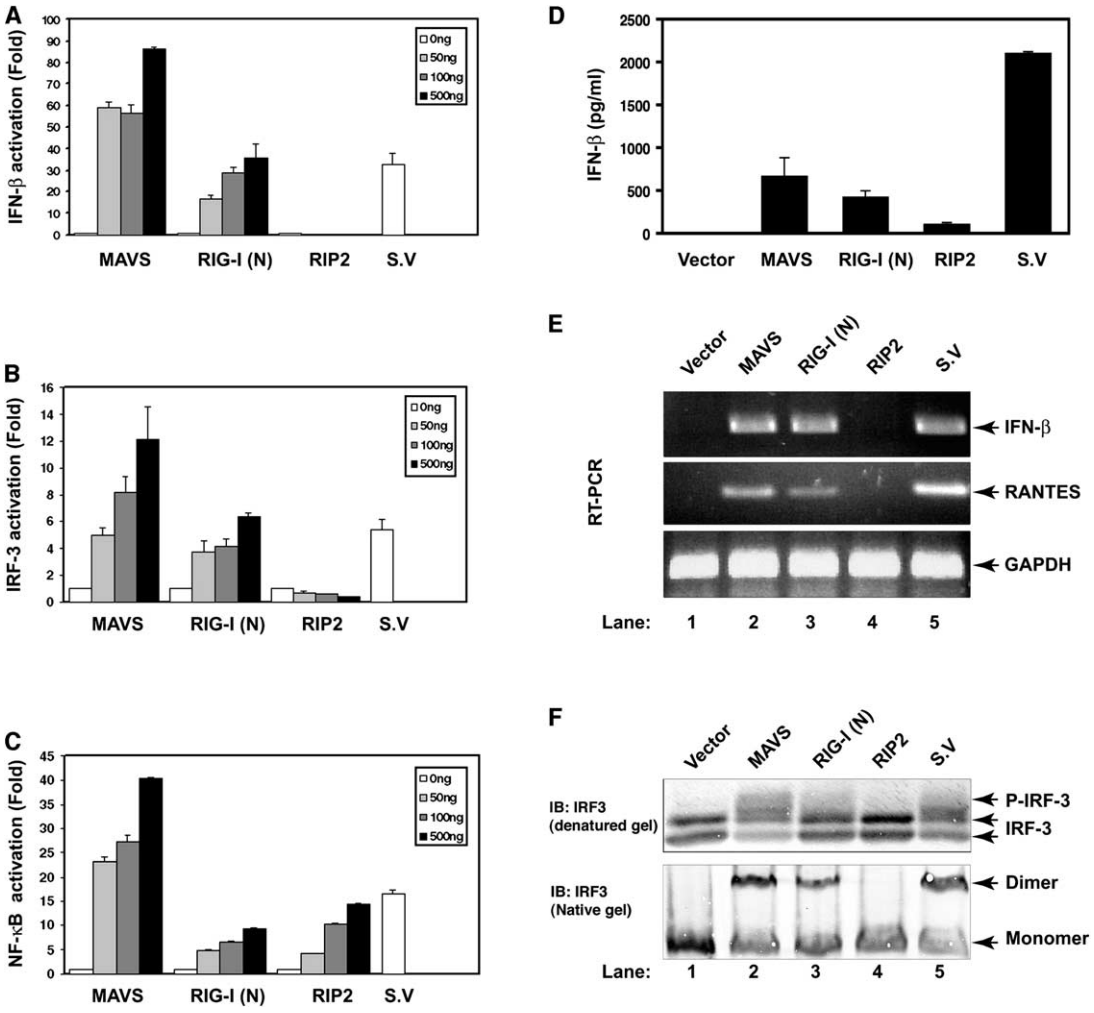

Figure 2. MAVS Is a Potent Inducer of IFN-β

(A) Increasing amounts of expression vectors for MAVS, RIG-I(N), and RIP2 were transfected into HEK293 cells together with an IFNβ-luciferase reporter as well as pCMV-LacZ as an internal control. Thirty-six hours after transfection, the luciferase activity was measured and normalized based on β-galactosidase activity. The error bars represent the standard deviation from the mean value obtained from duplicated experiments. S.V.: cells transfected with IFNβ-Luc were infected with Sendai virus for 20 hr.

(B) The experiments were carried out as in (A), except that Gal4-Luc and Gal4-IRF3 plasmids were cotransfected together in lieu of IFNβ-Luc.

(C) Similar to (A), except that p-κB_3-tk-Luc was transfected in lieu of INFβ-Luc.

(D) HEK293 cells were transfected with the expression vectors for MAVS (500 ng), RIG-I(N; 200 ng), RIP2 (500 ng), the vector pcDNA3 (500 ng), or infected with Sendai virus (S.V.; 50 HA units/ml). Thirty-six hours after transfection or 20 hr after viral infection, the culture supernatant was collected to measure IFN-β production by ELISA.

(E) An aliquot of the cell pellet from (D) was lysed to isolate RNA for RT-PCR using primers specific for IFN-β, the chemokine RANTES, and GAPDH (as a control).

(F) After transfection or viral infection as described in (D), HEK293 cells were lysed to prepare protein extracts, which were then resolved by SDS-PAGE (upper panel) or native gel electrophoresis (lower panel). Phosphorylation or dimerization of IRF3 was detected by immunoblotting (IB) with an IRF3 antibody.

noblotting in multiple human cell lines (Figure S2), including Jurkat (T cell), U937 (monocyte), Huh7 (hepatocyte), A549 (lung epithelial cell), and HeLa (cervical epithelial cell). Thus, MAVS is expressed in many different cell types, especially those that constitute the first line of defense against viruses, such as liver and lung cells.

Strikingly, both pairs of MAVS siRNA oligos abolished IFN-β induction by Sendai virus (Figure 3A, upper panel). Since the sequences of these two pairs of RNA oligos are very different, it is exceedingly unlikely that they silence a common "off-target" gene responsible for IFN-β induction. Further supporting this conclusion, we found that a MAVS expression vector containing a silent mutation that renders MAVS resistant to RNAi was able to rescue IFN-β induction in the MAVS RNAi cells (data not shown). As controls, RNAi of RIG-I, but not GFP, also blocked viral induction of INF-β (Figure 3A). Similarly, RNAi of MAVS or RIG-I blocked the production of endogenous IFN-β protein by Sendai virus,

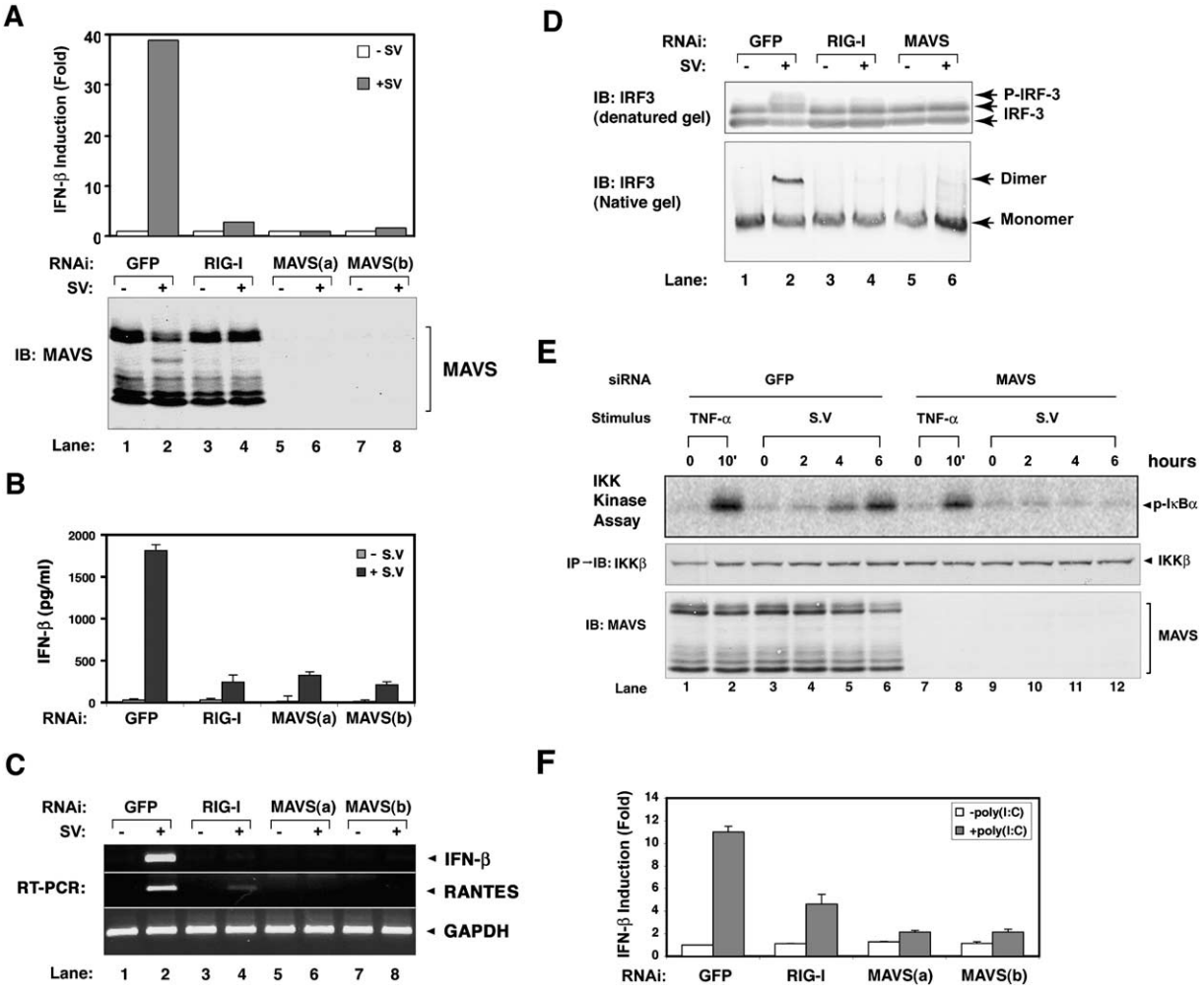

Figure 3. MAVS Is Required for IFN-β Induction by Sendai Virus

(A) siRNA oligos targeting GFP (control), RIG-I, and two different regions of MAVS (a and b) were transfected into HEK293 cells to silence the expression of endogenous proteins. The efficiency of MAVS RNAi was confirmed by immunoblotting with a MAVS-specific antibody (bottom panel). To measure IFNβ induction, the IFNβ-Luc reporter plasmid was transfected into the RNAi cells, which were then infected with Sendai virus for 20 hr followed by luciferase assays (upper panel).

(B) The siRNA transfection into HEK293 cells and viral infection were carried out as in (A), and the supernatant was collected for measurement of IFN-β by ELISA.

(C) Similar to (B), except that cells were lysed to isolate RNA for RT-PCR.

(D) Similar to (B), except that protein extracts were prepared from the cells and analyzed for IRF3 phosphorylation by SDS-PAGE (upper panel) or dimerization by native gel electrophoresis (lower panel).

(E) MAVS is required for IKK activation by Sendai virus. HEK293 cells expressing the full-length RIG-I, which facilitates the activation of IKK and IRF3 by Sendai virus, were transfected with siRNA oligos for GFP or MAVS. These cells were then stimulated with TNFα (10 ng/ml) or infected with Sendai virus (50 HA units/ml) for the indicated time before cell lysates were prepared. An aliquot of the cell lysates (20 μg) was immunoblotted with a MAVS antibody (lower panel). Five hundred micrograms of the cell lysates were immunoprecipitated with an antibody against NEMO to isolate the IKK complex, whose activity was measured using GST-IκBα and γ-^{32}P-ATP as substrates (upper panel). An aliquot of the IKK immunoprecipitate was immunoblotted with an IKKβ antibody (middle panel).

(F) MAVS is required for IFN-β induction by double-stranded RNA. HEK293-RIGI cells were transfected with siRNA oligos targeting GFP, RIG-I, or MAVS as described in (A). Subsequently, cells were transfected with 0.5 μg of poly(I:C) or pcDNA3 (as control) together with the IFNβ-Luc and pCMV-LacZ plasmids. Luciferase assays were performed 48 hr after transfection.

as measured by ELISA (Figure 3B). RT-PCR analyses showed that viral induction of IFN-β and RANTES RNA was abolished in the absence of MAVS or RIG-I (Figure 3C). Furthermore, RNAi of MAVS or RIG-I prevented the phosphorylation (Figure 3D, upper panel) and dimerization (Figure 3D, lower panel) of IRF3 induced by Sendai virus, indicating that both MAVS and RIG-I are required for IRF3 phosphorylation. To determine if MAVS is also required for IKK activation by the virus, we carried out an IKK kinase assay (Figure 3E). Since the activation of IKK by Sendai virus is much slower and weaker as compared to TNFα stimulation, we transfected HEK293 cells with an expression construct encoding the full-length RIG-I protein, which potentiated the activation

of IKK such that IKK activity was detectable within 4 hr of viral infection (Figure 3E, lanes 3–6). Importantly, RNAi of MAVS blocked IKK activation by Sendai virus, but not TNFα. To determine if MAVS is required for interferon-β induction by dsRNA, we transfected poly(I:C) into a HEK293 cell line stably expressing the full-length RIG-I protein. The transfected poly(I:C) is known to mimic viral dsRNA to bind to RIG-I and stimulate interferon production. As shown in Figure 3F, knockdown of MAVS expression with two different pairs of siRNA oligos blocked IFN-β induction by poly(I:C), suggesting that MAVS may be required for immune defense against all RNA viruses that generate dsRNA in their life cycle. Taken together, these results demonstrate that MAVS is essential for viral activation of IKK and IRF3.

MAVS Is a Potent Antiviral Protein

Since MAVS is both necessary and sufficient for the induction of type-I interferons, we examined whether this protein could mediate immune defense against the vesicular stomatitis virus (VSV), an RNA virus of the rhabdoviridae family. Infection of HEK293 cells by VSV led to nearly complete killing of the cells within 24 hr at a multiplicity of infection (MOI) of 0.01 (Figure 4A). Transfection of these cells with an expression vector encoding FLAG-MAVS prevented cell killing by VSV even at a MOI of 0.1. Conversely, silencing of the endogenous MAVS expression by RNAi greatly sensitized cell killing by VSV at a much lower MOI (0.001). Measurement of the viral titer showed that overexpression of FLAG-MAVS decreased the viral titer by more than 20-fold as compared to control cells (from 5.5×10^7 to 2.6×10^6 plaque-forming units [pfu] at 12 hr after infection; Figure 4B). Conversely, RNAi of MAVS led to an increase of viral titer by 20-fold as compared to control cells (from 5.5×10^7 to 1.1×10^9 pfu). These results show that MAVS is a pivotal cellular antiviral protein whose expression level directly determines antiviral immunity.

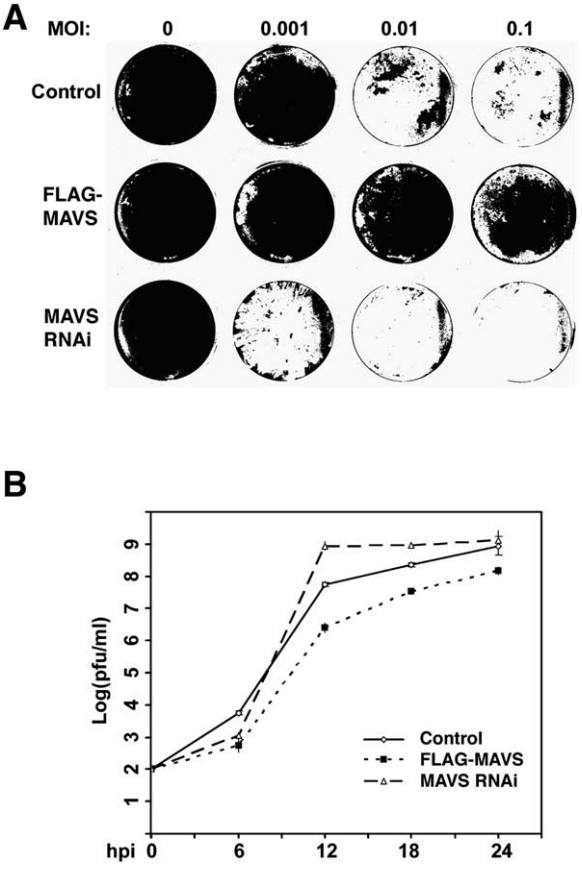

Figure 4. MAVS Is a Potent Antiviral Protein

(A) HEK293 cells were transfected with pcDNA3-FLAG-MAVS (0.5 μg) or siRNA oligos (20 nM) targeting MAVS. Forty-eight hours after transfection, cells were infected with VSV at the indicated MOI for 24 hr. After fixing, cells that were not killed by the virus were stained with Amido black.

(B) The culture supernatant from cells infected with VSV at the MOI of 0.01 were collected at the indicated time points, and the viral titer was determined by plaque assay.

MAVS Functions Downstream of RIG-I and Upstream of TBK1

As both RIG-I and MAVS function upstream of IKK and IRF3 activation, we sought to determine the epistatic relationship between these two proteins. As shown in Figure 5A, RNAi of MAVS blocked IFN-β induction by Sendai virus, or by overexpression of the N-terminal fragment of RIG-I (RIG-I(N)) as well as MAVS itself. In contrast, RNAi of RIG-I did not inhibit IFN-β induction by the overexpression of MAVS. This pair of siRNA oligos blocked INF-β induction by Sendai virus, but not RIG-I(N), because the sequence targeted by the RNA oligos was located at nucleotides 2363–2381, outside the region encoding RIG-I(N). Similar to IFN-β, the IRF7-mediated induction of IFN-α by Sendai virus also required RIG-I and MAVS (Figure 5B). Furthermore, RNAi of MAVS blocked IFN-α activation by RIG-I(N). In contrast, RNAi of RIG-I did not affect IFN-α induction by MAVS (Figure 5B). We conclude from these experiments that MAVS functions downstream of RIG-I in the antiviral signaling pathway.

Recent studies have shown that overexpression of TRIF, TBK1, or IKKε is sufficient to activate IFN-β and that TBK1 and IKKε are the kinases that phosphorylate IRF3 at the C terminus. We therefore investigated the relationship between MAVS and TRIF, TBK1, and IKKε. While RNAi of MAVS abolished IFN-β induction by Sendai virus, it had no effect on the activation of IFN-β by TRIF, TBK1, or IKKε (Figure 5C). Consistent with previous reports, RNAi of RIG-I did not affect IFN-β induction by TRIF, TBK1, or IKKε (Yoneyama et al., 2004). These results indicate that RIG-I and MAVS do not function downstream of TRIF, TBK1, or IKKε. To determine if TBK1 or IKKε functions downstream of MAVS, we attempted to knock down the expression of TBK1 and IKKε by RNAi in HEK293 cells. We have tried nine different pairs of TBK1 and five different pairs of IKKε siRNA oligos individually or in combination. Unexpectedly, none of the TBK1 and/or IKKε siRNA oligos blocked IFN-β induction by MAVS or Sendai virus (data not shown). Since we cannot rule out the possibility that the RNAi experiments did not result in sufficient knockdown of TBK1 or IKKε protein, we turned to TBK1-deficient MEF cells, which are known to be de-

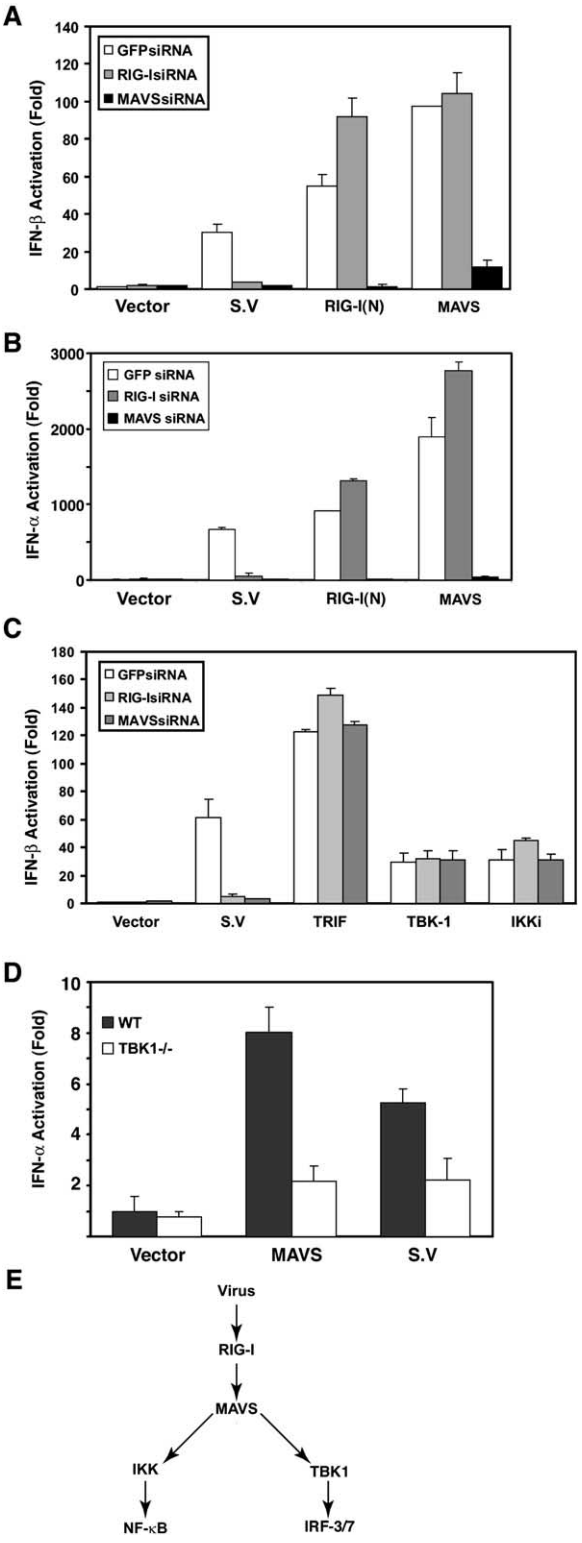

Figure 5. MAVS Functions Downstream of RIG-I and Upstream of TBK1

(A) HEK293 cells were transfected with siRNA oligos targeting GFP, RIG-I, or MAVS. These cells were subsequently transfected with IFNβ-Luc together with expression vectors (300 ng) encoding the N-terminal fragment of RIG-I [RIG-I(N)], MAVS, or empty vector (pcDNA3). As a positive control, cells were infected with Sendai virus (S.V.). Twenty hours after viral infection or 24 hr after transfection of the expression plasmids, cells were harvested for luciferase assays.

(B) Similar to (A) except that pIFNα4-Luc (40 ng) and pcDNA3-FLAG-IRF7 (10 ng) were transfected into HEK293 cells to measure the activation of IFNα by IRF7.

(C) Similar to (A) except that expression vectors (300 ng) for TRIF, TBK1, and IKKε were used.

(D) Wild-type or TBK1$^{-/-}$ MEF cells were transfected with pIFNα4-Luc (300 ng) and pcDNA3-FLAG-IRF7 (50 ng) together with pEF-HA-MAVS (100 ng) or control vector. For Sendai virus infection, MEF cells transfected with the luciferase reporter plasmids were infected with 50 HA units/ml of the virus.

(E) A proposed antiviral signaling pathway. In this pathway, MAVS functions downstream of RIG-I and upstream of IKK and TBK1.

fective in producing interferons in response to Sendai virus infection. As shown in Figure 5D, infection of Sendai virus or overexpression of MAVS induced IFN-α in the wild-type MEF cells. In contrast, the IFN-α induction was greatly reduced in TBK1-deficient cells. Collectively, the results shown in Figures 3D, 3E, and 5 delineate a signaling pathway in which MAVS functions downstream of RIG-I and upstream of IKK and TBK1 (Figure 5E).

The CARD-like Domain Is Essential for MAVS Signaling

The N-terminal CARD-like domain of MAVS is evolutionarily conserved (Figure 1C). In addition, MAVS contains a proline-rich domain in the middle (Figure 1A). To investigate the functions of these domains, we engineered expression constructs encoding MAVS mutant proteins lacking either the CARD-like domain (ΔCARD) or the proline-rich domain (ΔPRO; Figure 6A). As shown in Figures 6B and 6C, deletion of the CARD-like domain, but not the proline-rich domain, abolished the ability of MAVS to activate IFN-β or NF-κB. Furthermore, a point mutation of a conserved threonine residue to alanine (T54A) or simultaneous mutations of three conserved residues in the CARD-like domain to alanine (G67A/W68A/V69A, abbreviated as AAA) severely impaired the ability of MAVS to activate IFN-β (Figure 6D). These results indicate that an intact CARD-like domain is essential for MAVS signaling. This conclusion was further supported by Figures 6E and 6F, which showed that MAVS-ΔCARD, but not MAVS-ΔPRO, functioned as a dominant-negative mutant that inhibited the activation of IFN-β and NF-κB promoters by Sendai virus. The CARD-like domain alone did not function as a dominant-negative mutant (Figure S3), suggesting that when the CARD-like domain is not tethered to the rest of MAVS protein such as the membrane domain, it may not interact effectively with other proteins in the pathway.

The C-Terminal Transmembrane (TM) Domain of MAVS Is Essential for Its Function

Notably, the C terminus of MAVS contains a conserved hydrophobic transmembrane (TM) domain, which resembles the TM domain of several tail-anchored mitochondrial proteins, including the proteins of the Bcl-2 family that protect cells from undergoing apoptosis

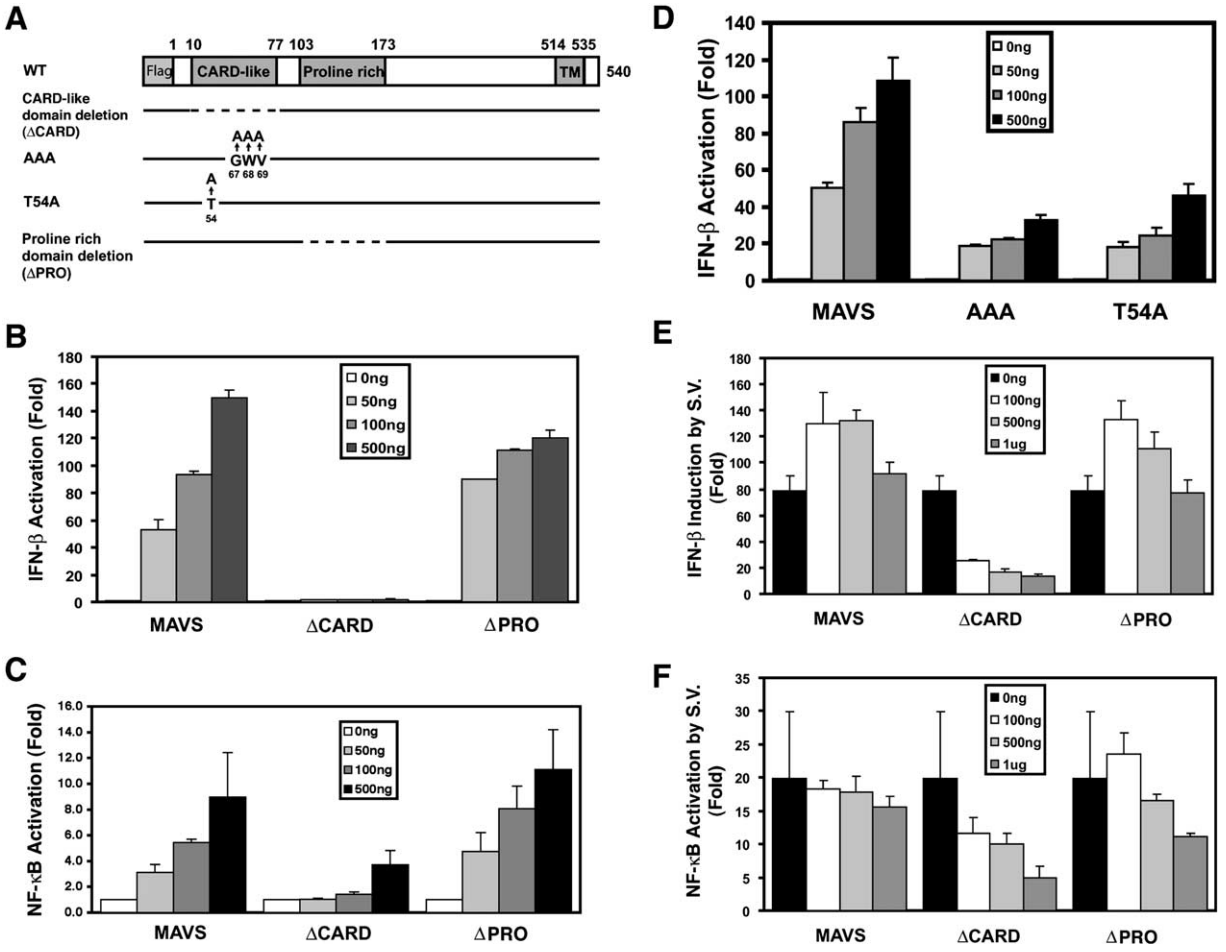

Figure 6. The CARD-like Domain Is Essential for MAVS Signaling

(A) A diagram illustrating the MAVS mutants. ΔCARD: lacking residues 10–77; ΔPRO: lacking residues 103–152; AAA: G67A/W68A/V69A.

(B–D) HEK293 cells were transfected with IFNβ-Luc or κB3-Luc together with expression vectors for MAVS and its mutants as indicated.

(E) The ΔCARD mutant of MAVS is a dominant-negative inhibitor of IFN-β induction by Sendai virus. HEK293 cells were transfected with IFNβ-Luc together with expression vectors for MAVS or its mutants. The cells were then infected with Sendai virus for 20 hr followed by measurement of luciferase activity.

(F) Similar to (E), except that κB3-Luc was used in lieu of IFNβ-Luc.

(Figure 7A, left panel; Kaufmann et al., 2003). To determine the function of this domain, we created a MAVS mutant protein lacking the C-terminal TM domain (MAVS-ΔTM). This mutant protein completely lost its ability to activate IFN-β (Figure 7A, right panel). Immunoblotting experiments showed that MAVS-ΔTM was abundantly expressed and became a soluble cytosolic protein, whereas the full-length MAVS was present in membrane pellets (data not shown; also see Figure 7C for confocal image).

The CARD-like and TM Domains of MAVS Are Sufficient to Induce IFN-β

Since the most conserved regions of MAVS are the N-terminal CARD-like domain and the C-terminal TM domain, and each of these domains is necessary for MAVS signaling, we examined whether these two domains are sufficient to activate IFN-β expression. Remarkably, the MAVS mutant containing only the CARD-like and TM domains (N100 + TM) was sufficient to induce IFN-β (Figure 7B), whereas the mutants containing only the CARD-like domain were inactive. Thus, the CARD-like and TM domains are both necessary and sufficient for MAVS signaling.

MAVS Is a Mitochondrial Membrane Protein

To determine the subcellular localization of MAVS, we employed confocal microscopy to image HeLa cells transfected with an expression vector encoding HA-tagged MAVS (Figure 7C, upper panel). Fluorescent immunostaining with an HA-specific antibody showed a punctate pattern of MAVS localization that overlapped with the staining pattern of Mito Tracker, a fluorescent marker taken up specifically by mitochondria. We also found by confocal microscopy that MAVS lacking the C-terminal transmembrane domain (MAVS-ΔTM) was a cytosolic protein that no longer overlapped with Mito Tracker staining (Figure 7C, lower panel). As

the C-terminal TM domain of MAVS is similar to that of Bcl-2, which is localized to both endoplasmic reticulum (ER) and mitochondria, we examined whether a fraction of MAVS might be localized to ER. As shown in Figure S4A, the staining pattern of MAVS did not overlap with that of the ER marker calnexin, indicating that MAVS is predominantly not an ER protein. To localize the endogenous MAVS protein, we used the affinity-purified MAVS antibody for imaging (Figure S4B). Similar to the transfected HA-MAVS, the endogenous MAVS also showed a punctate staining pattern that overlapped with the staining of cytochrome c, a well-known mitochondrial protein. Although the resolution of confocal microscopy did not allow for the precise localization of MAVS at the ultrastructural level within the mitochondria, these experiments clearly show that MAVS is localized to the mitochondria.

To further determine if MAVS is localized to the mitochondrial membrane, we carried out subcellular fractionation experiments. HEK293 cells were homogenized in an isotonic buffer that preserved mitochondria and other organelles, and the cell lysates were then subjected to differential centrifugation to separate nuclei, mitochondria, and other organelles as well as cytosol (Figure 7D). MAVS was found in the 5000 × g pellet (P5), together with other mitochondrial proteins including Bcl-xL and cytochrome c oxidase (COX). Immunoblotting with an antibody against the endosomal protein EEA-1 showed that the distribution of this protein did not correlate with that of MAVS. Similarly, the markers of endoplasmic reticulum (BiP) and lysosome (LAMP-1) did not cosegregate with MAVS (data not shown).

To determine whether MAVS is localized in the outer or inner mitochondrial membrane, the mitochondrial fraction (P5) was sonicated to partially rupture the outer mitochondrial membrane and then fractionated by sucrose gradient ultracentrifugation (Figure 7D). The sonication released cytochrome c from the intermitochondrial membrane space and resulted in a small fraction of outer mitochondrial membrane floating on the top of the sucrose gradient, as indicated by immunoblotting with an antibody against Bcl-xL, which is predominantly located in the outer mitochondrial membrane. Under the same condition, the inner mitochondrial membrane protein COX remained largely in the dense fractions of the sucrose gradient. Interestingly, a small fraction of MAVS comigrated with Bcl-xL to the lighter membrane fractions, suggesting that MAVS colocalizes with Bcl-xL in the outer mitochondrial membrane. This conclusion was further supported by our observation that MAVS and Bcl-xL could be extracted from the mitochondrial membrane with the same concentration of Triton X-100 (0.1%), whereas the extraction of COX requires higher Triton X-100 concentration (0.2%, data not shown).

Mislocalization of MAVS Impairs Its Function

The aforementioned experiments showed that MAVS is predominantly localized to the mitochondrial membrane (Figures 7C and 7D), and that removal of the mitochondrial targeting sequence abolishes its activity (Figures 7A and 7B). To further examine the importance of mitochondrial localization for MAVS function, we replaced the C-terminal TM domain of MAVS with peptide sequences that target MAVS to different membrane locations. These sequences include the CAAX motif from Rac1 that is known to target fusion proteins predominantly to the plasma membrane (Michaelson et al., 2001); the ER targeting sequence from VAMP-2 (vesicle associated membrane protein-2), which is predominantly an ER membrane protein (Kim et al., 1999); the TM sequence from Bcl-2, which is localized in both ER and mitochondria (Kaufmann et al., 2003); and the TM sequence from Bcl-xL, which is predominantly in the mitochondrial outer membrane (Kaufmann et al., 2003). As shown in Figure 7E, replacement of the TM domain of MAVS with the analogous domain from Bcl-2 or Bcl-xL did not impair the ability of MAVS to induce IFN-β. In contrast, the mislocalization of MAVS to the plasma membrane (CAAX) or ER (VAMP-2) markedly reduced the activity of MAVS. Confocal microscopy experiments confirmed that the majority of MAVS fusion proteins containing the CAAX or VAMP-2 targeting sequences were no longer present in the mitochondria, whereas the fusion proteins containing the Bcl-2 or Bcl-xL targeting sequences were predominantly in the mitochondria (Figure S4C). The residual activity (20%–30% of the wild-type MAVS) may be due to incomplete mislocalization of the overexpressed MAVS proteins. Taken together, these results clearly demonstrate the importance of mitochondrial localization for the signaling function of MAVS.

MAVS Is Resistant to Detergent Extraction from Membranes Following Viral Infection

Since we did not detect any difference of MAVS protein at the level of expression or modification after viral infection, we sought to examine whether the localization of MAVS changes in response to viral infection. We found that Sendai virus did not cause the translocation of MAVS from mitochondria to cytosol (data not shown). However, when the mitochondrial fraction (P5) was further extracted with 0.5% Triton X-100, the majority of MAVS was extracted from mitochondrial membranes isolated from mock-infected cells, but not from viral-infected cells. In fact, MAVS was even resistant to extraction with 1% Triton X-100 following viral infection (data not shown). These results suggest that MAVS translocates to a detergent-resistant membrane domain or particle following viral infection. Further studies are required to determine the precise location to which MAVS emigrates and whether this new localization triggers antiviral immune response.

Discussion

In this report, we describe the identification of MAVS as a novel cellular protein essential for innate immune defense against viruses. We show that overexpression of MAVS is sufficient to activate the NF-κB, IRF3, and IRF7 pathways to induce type-I interferons including IFN-α and IFN-β, which inhibit viral replication. Conversely, silencing of endogenous MAVS expression by RNAi abolishes the activation of NF-κB, IRF3, and IRF7, thus blocking the production of interferons and permit-

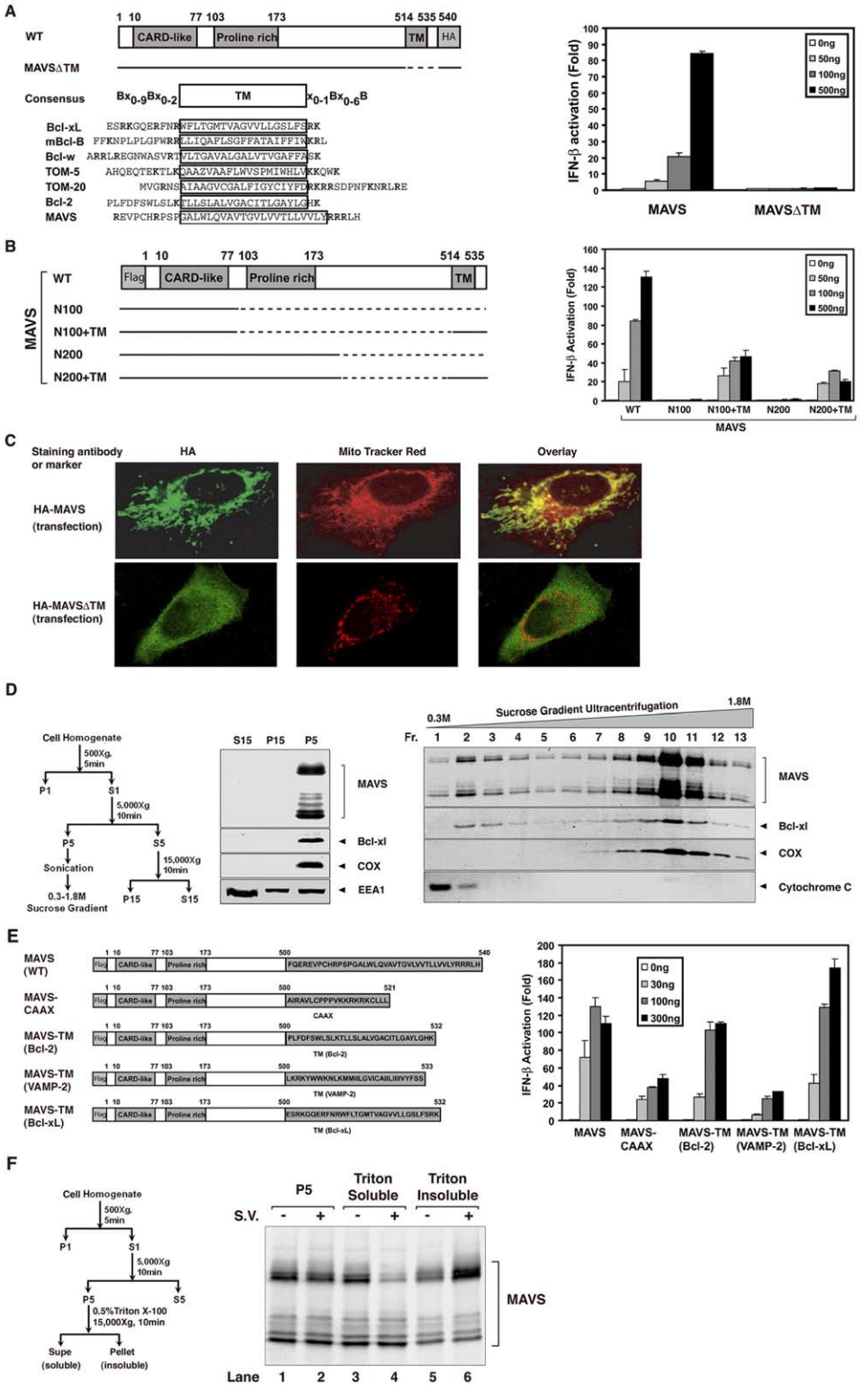

Figure 7. MAVS Is a Mitochondrial Antiviral Signaling Protein

(A) MAVS contains a mitochondrial membrane targeting sequence that is essential for signaling. The left panel shows the alignment of the MAVS transmembrane (TM) sequence with those of known mitochondrial membrane proteins, including proteins of the Bcl-2 family. The MAVS mutant lacking the C-terminal 30 residues (ΔTM) is illustrated. This mutant or wild-type (wt) MAVS was transfected into HEK293 cells together with IFNβ-Luc to measure IFN-β induction (right panel).

(B) A MAVS mutant containing the CARD and TM domain is sufficient to activate IFN-β. The MAVS mutants are illustrated on the left panel. These mutants were transfected into HEK293 cells together with IFNβ-Luc to measure IFN-β induction (right panel).

ting viral infection. Epistasis experiments show that MAVS functions downstream of the viral RNA receptor RIG-I and upstream of IκB and IRF3 phosphorylation. MAVS contains an N-terminal CARD-like domain and a C-terminal mitochondrial membrane-targeting domain, both of which are essential for MAVS signaling. The mitochondrial localization of MAVS is particularly interesting, as this is the first example of a mitochondrial protein playing a pivotal role in innate immunity. To our knowledge, MAVS is also the first mitochondrial protein known to activate NF-κB and IRF transcription factors.

The N-terminal CARD-like domain of MAVS likely mediates its interaction with other CARD-containing proteins. The logical candidates of MAVS-interacting proteins include the CARD-like domain proteins RIG-I and MDA-5. Indeed, we were able to detect weak but reproducible binding between MAVS and RIG-I in coimmunoprecipitation experiments when these proteins were overexpressed together (Figure S5A). However, we have not been able to detect any direct interaction between endogenous MAVS and RIG-I in the presence or absence of viral infection, nor have we observed translocation of RIG-I to the mitochondria following viral infection. Both RIG-I and MDA-5 contain two CARD-like domains, which may interact with each other intramolecularly, thus preventing their interaction with other CARD domain proteins. The binding of viral RNA to the C-terminal RNA helicase domain of RIG-I may induce a conformational change that allows the tandem CARD domains of RIG-I to interact with MAVS directly or indirectly. More extensive studies are required to determine the validity and functional significance of interaction between RIG-I and MAVS.

How MAVS activates NF-κB and IRF3 is currently unknown. The NF-κB pathway is primarily regulated by the activation of IKK, which integrates signals from multiple pathways. The mechanisms of IKK activation by extracellular ligands such as TNFα and IL-1β have been extensively studied (Sun and Chen, 2004). In these pathways, several proteins including TRAF2, TRAF6, RIP1, TAK1, and TAB2 have been shown to be important for IKK activation. We have examined the potential interaction of these proteins with MAVS and found that only TRAF6 could weakly associate with MAVS (Figure S5A), presumably through a putative TRAF6 binding sequence in the proline-rich region of MAVS (PGENSE, residues 153–158; Ye et al., 2002). However, deletion of this region had no effect on the ability of MAVS to induce IFN-β (Figure 6B) or NF-κB (Figure 6C). Furthermore, IFN-β induction by Sendai virus was not impaired in TRAF6-deficient MEF cells (Figure S5B). Consistent with our results, Gohda et al. (2004) have recently shown that TLR3 signaling and IFN-β induction by LPS are normal in TRAF6-deficient macrophages. Recently, it has been shown that RIP1 and FADD are involved in viral induction of IFN-β (Balachandran et al., 2004), raising the possibility that these proteins mediate signaling by MAVS. However, we did not detect any interaction between MAVS and RIP1 or FADD (Figure S5A). Furthermore, the RIP1-deficient MEF cells were fully capable of producing IFN-β in response to Sendai virus infection (Figure S5B). We have also been unable to detect any direct interaction between MAVS and any subunit of the IKK complex, including IKKα, IKKβ, and NEMO. Thus, it appears that none of the proteins known to be involved in the classical pathways of IKK activation is a direct link between MAVS and IKK activation.

The localization of MAVS to the mitochondria provides a strategic position to detect viral replication, which often occurs in intracellular organelles such as ER. For example, the replication of hepatitis C virus (HCV) RNA occurs in a membranous web that connects ER and mitochondria (Rehermann and Nascimbeni, 2005). The HCV core protein has also been found to reside in the mitochondrial membrane (Schwer et al., 2004). The dsRNA, which is present in the viral RNA-protein particles, may recruit the RNA helicase RIG-I and MDA-5 to the membranous web, allowing these proteins to interact with MAVS directly or indirectly. The signal of viral replication may then be transmitted to the mitochondria, which triggers antiviral responses through activation of NF-κB and IRF3.

Mitochondria represent the best example of harmonious symbiosis between the ancient bacteria and eukaryotic cells. From this bacterial origin, mitochondria have further evolved as a sentinel of intrinsic and extrinsic stress or insults to the cell. The role of mitochondria in apoptosis is an excellent example of how mitochondria govern the homeostasis and wellness of an organism by regulating cell death in response to stress signals (Wang, 2001). Several apoptotic and antiapoptotic proteins are localized to the mitochondria. The first mitochondrial protein known to be involved in apoptosis is the protooncogene Bcl-2 (Hockenbery et al., 1990), which has a C-terminal mito-

(C) MAVS is a mitochondrial protein. pEF-HA-MAVS was transfected into HeLa cells, which were then stained with an HA antibody and imaged by confocal microscopy. The mitochondria were stained with Mito Tracker. The yellow staining in the overlay image indicates colocalization of MAVS and Mito Tracker.

(D) Subcellular fractionation of MAVS. HEK293 cells were homogenized in an isotonic buffer and then subjected to differential centrifugation as shown in the diagram. Different fractions as indicated were analyzed by immunoblotting with antibodies against MAVS, Bcl-xL (outer mitochondrial membrane), COX (inner mitochondrial membrane), and EEA1 (endosome marker). On the right panel, the crude mitochondrial fraction (P5) was sonicated to disrupt the outer mitochondrial membrane and then fractionated by sucrose gradient ultracentrifugation. The fractions were immunoblotted with the indicated antibodies.

(E) Mislocalization of MAVS impairs its function. Expression vectors for the MAVS fusion proteins as indicated on the left panel were transfected into HEK293 cells together with IFNβ-Luc to measure IFN-β induction (right panel). The expression levels and subcellular localization of the MAVS fusion proteins are shown in Figures S4C and S4D.

(F) MAVS translocates to a detergent insoluble membrane domain following viral infection. The mitochondrial fraction (P5) isolated from mock- or viral-infected HEK293 cells was resuspended in a buffer containing 0.5% Triton X-100, and the detergent soluble and insoluble materials were then analyzed by immunoblotting for the presence of MAVS.

chondrial transmembrane domain similar to that of MAVS. In normal cells, the Bcl-2 family of proteins prevents the release of proapoptotic molecules such as cytochrome c and SMAC/DIABLO from the mitochondria to the cytoplasm. In response to an apoptotic stimulus such as DNA damage, cytochrome c and SMAC are released to the cytosol to initiate a caspase cascade leading to cell death. It is not clear whether MAVS activates NF-κB and IRF3 by mobilizing other mitochondrial components or through direct interaction with proteins functioning in the NF-κB and IRF3 pathways. Although much more work is required in order to elucidate the biochemical mechanism of MAVS signaling, our studies have uncovered a new role of mitochondria in innate immunity against pathogenic insults such as viral infection. Thus, mitochondria may have a central role in integrating signals from pathogenic challenge and orchestrating an immune or apoptotic response depending on the challenge. In this regard, members in several families of proteins involved in cell death have recently been shown to function in the immunity pathways. Examples of these proteins include caspase-8/Dredd, IAPs, and paracaspase (e.g, MALT1; van Oers and Chen, 2005). The CARD domain proteins, including APAF1, NOD1, NOD2, RIP2, RIG-I and now MAVS, represent another example of proteins that have pivotal functions in apoptosis as well as immunity. MAVS is particularly unique in that it is a CARD domain protein localized in the mitochondrial membrane, suggesting that it may also be involved in apoptosis. Indeed, our preliminary studies suggest that RNAi of MAVS in HEK293 cells led to a partial cleavage of PARP (POLY (ADP-ribose) polymerase; Figure S6), an early marker of apoptosis, suggesting that MAVS may protect cells from apoptosis. Thus, unlike other antiviral mechanisms that trigger the apoptosis of infected cells to limit viral spread, MAVS may help the survival of infected cells while mounting a potent interferon response to clear viral infection.

We have shown that higher expression of MAVS endows cells with stronger immunity to viral infection, whereas the loss of MAVS expression renders cells vulnerable to viral killing. These results raise the possibility that variations in the expression levels of MAVS may endow different individuals with differential immunity against viral diseases. As many viruses have evolved to acquire strategies to evade host immunity, it is quite possible that some viruses may target MAVS in order to achieve successful infection. In these cases, therapies that enhance MAVS expression or activity may be a viable option for achieving beneficial immune responses against viral diseases.

Experimental Procedures

Plasmids and Cell Lines

MAVS sequence was amplified by PCR using the IMAGE clone 5751684 (ATCC) as a template. PCR primers were based on GenBank accession number BC044952. The open reading frame of MAVS was cloned into the XhoI and MluI sites of the mammalian expression vector pEF-IRES-Puro such that N-terminal HA-tagged MAVS can be expressed under the control of EF1α promoter. pcDNA3-FLAG-MAVS was constructed by cloning MAVS into the XhoI and XbaI sites of pcDNA3. Truncated forms of MAVS lacking either the CARD-like domain (residues 10–77) or the proline-rich region (residues 103–152) were cloned into pcDNA3 using overlap extension PCR. A similar PCR strategy was used to generate MAVS mutants lacking the intervening sequence between the CARD and TM domains (N100 + TM and N200 + TM). To replace the TM domain of MAVS with another domain that targets the fusion protein to distinct membrane locations, the following sequences were used: CAAX (residues 128–148 of Rac1), VAMP-2 (residues 84–116), Bcl-2 (residues 208–239), and Bcl-xL (residues 202–233). These sequences were fused to the C terminus of MAVS (residues 1–500) using overlap extension PCR. Point mutations within the CARD-like domain of MAVS were introduced using the QuickChange kit (Strategene). pEF-BOS-FLAG-RIG-I and RIG-I(N) were kindly provided by Dr. Takashi Fujita (Tokyo Metropolitan Institute of Medical Science). cDNA encoding amino acids 1–242 of RIG-I was amplified by PCR and cloned into the XhoI and MluI sites of the baculoviral expression vector pFastBac (Invitrogen). For the expression of a MAVS protein fragment containing residues 131–291, the cDNA encoding this fragment was inserted into the NdeI and BamHI sites of pET14b (Novagen). The reporter gene IFNβ-Luc was constructed by subcloning 110 base pairs of the interferon-β promoter into a luciferase expression vector. All constructs were verified by automated DNA sequencing. Plasmids for p-κB_3-TK-Luc and pCMV-LacZ have been described previously (Deng et al., 2000). Plasmids for Gal4-Luc, Gal4-IRF3, Flag-TRIF, Flag-TBK1, and Flag-IKKε were provided by Dr. Kate Fitzgerald (University of Massachusetts, Worcester) and Dr. Tom Maniatis (Harvard). The IRF7 and IFN-α4-Luc plasmids were from Dr. John Hiscott (McGill University), and pcDNA3-myc-RIP2 was from Dr. Gabriel Nunez (University of Michigan). The MEF cell lines deficient in TRAF6, RIP1, and TBK1 were provided by Drs. Jun-Ichiro Inoue (University of Tokyo), Michelle Kelliher (University of Massachusetts, Worcester) and Wen-Chen Yeh (University of Toronto), respectively.

Antibodies and Proteins

The antibodies against RIG-I and MAVS were generated by immunizing rabbits with the recombinant proteins His_6-RIG-I (1–242) produced in Sf9 cells and His_6-MAVS (131–291) produced in *E. coli*, respectively. Both antibodies were affinity purified using the respective RIG-I and MAVS antigen column. Rabbit polyclonal antibody against IRF3 (SC-9082) and NEMO (SC-8330) were purchased from Santa Cruz Biotechnology. Monoclonal antibody against IKKβ (BD Bioscience), FLAG (M2; Sigma), HA.11 (Covance), Calnexin (Stressgen), phospho-JNK, and PARP (Cell Signaling) were purchased from the indicated suppliers.

RNAi

siRNA oligos at a final concentration of 20 nM were transfected into HEK293 cells using the calcium phosphate precipitation method. This transfection procedure was repeated on the second day to increase RNAi efficiency. On the third day, cells were transfected with indicated expression plasmids using Lipofectamine 2000 reagent (Invitrogen), and harvested 24 hr later. The sequences of the siRNA oligos are as follows (only the sense strands are shown): GFP (471–489), GCAGAAGAACGGCAUCAAG; RIG-I (2363–2381), AAUUCAUCAGAGAUAGUCA; MAVSa (899–917), CCACCUU GAUGCCUGUGAA; MAVSb (1364–1382): CAGAGGAGAAUGAGUA UAA. These RNA oligos were synthesized at the UT Southwestern Center for Biomedical Invention (CBI) facility.

Confocal Imaging

HeLa cells were transfected with Polyfect reagent (Qiagen). Twenty-four hours later, cells were trypsinized and plated onto coverslips in 24-well plates. After allowing the cells to adhere for 12–18 hr, cells were incubated with 250 nM Mito Tracker Red (Molecular Probes) for 30 min at 37°C. Cells on the coverslips were then washed once with PBS and fixed in 3.7% formaldehyde in PBS for 15 min. Cells were permeabilized and blocked for 30 min at room temperature in a staining buffer containing Triton X-100 (0.2%) and BSA (3%), and then incubated with a primary antibody in the staining buffer lacking Triton X-100 for 1 hr. After washing three times in the staining buffer lacking Triton X-100, cells were incubated with a secondary antibody for 1 hr. The coverslips, which were washed extensively, were dipped once in water and mounted onto slides

using mounting media (VectaShield; Vector Laboratories). Imaging of the cells was carried out using Zeiss LSM510 META laser scanning confocal microscopy.

Please refer to the Supplemental Data for additional Supplemental Experimental Procedures.

Supplemental Data

Supplemental Data include six figures and Supplemental Experimental Procedures and can be found with this article online at http://www.cell.com/cgi/content/full/122/5/669/DC1/.

Acknowledgments

We thank Drs. Takashi Fujita, Kate Fitzgerald, Tom Maniatis, Michael Gale, John Hiscott, and Gabriel Nunez for plasmids, and Drs. Jun-Ichiro Inoue, Wen-Chen Yeh, and Michelle Kelliher for the MEF cell lines. This work was supported by grants from NIH (RO1-AI60919), the Welch Foundation (I-1389), and the American Cancer Society (RSG0219501TBE). Confocal microscopy was supported by funding from an NIH shared instrumentation grant 1-S10-RR19406. Z.J.C. is a Leukemia and Lymphoma Society Scholar and a Burroughs Wellcome Fund Investigator in Pathogenesis of Infectious Diseases.

Received: June 8, 2005
Revised: August 8, 2005
Accepted: August 11, 2005
Published online: August 25, 2005

References

Akira, S., and Takeda, K. (2004). Toll-like receptor signalling. Nat. Rev. Immunol. *4*, 499–511.

Andrejeva, J., Childs, K.S., Young, D.F., Carlos, T.S., Stock, N., Goodbourn, S., and Randall, R.E. (2004). The V proteins of paramyxoviruses bind the IFN-inducible RNA helicase, mda-5, and inhibit its activation of the IFN-beta promoter. Proc. Natl. Acad. Sci. USA *101*, 17264–17269.

Baeuerle, P.A., and Baltimore, D. (1988). Activation of DNA-binding activity in an apparently cytoplasmic precursor of the NF-κ B transcription factor. Cell *53*, 211–217.

Balachandran, S., Thomas, E., and Barber, G.N. (2004). A FADD-dependent innate immune mechanism in mammalian cells. Nature *432*, 401–405.

Crozat, K., and Beutler, B. (2004). TLR7: a new sensor of viral infection. Proc. Natl. Acad. Sci. USA *101*, 6835–6836.

Darnell, J.E., Jr., Kerr, I.M., and Stark, G.R. (1994). Jak-STAT pathways and transcriptional activation in response to IFNs and other extracellular signaling proteins. Science *264*, 1415–1421.

Deng, L., Wang, C., Spencer, E., Yang, L., Braun, A., You, J., Slaughter, C., Pickart, C., and Chen, Z.J. (2000). Activation of the IκB kinase complex by TRAF6 requires a dimeric ubiquitin-conjugating enzyme complex and a unique polyubiquitin chain. Cell *103*, 351–361.

Fitzgerald, K.A., McWhirter, S.M., Faia, K.L., Rowe, D.C., Latz, E., Golenbock, D.T., Coyle, A.J., Liao, S.M., and Maniatis, T. (2003). IKKepsilon and TBK1 are essential components of the IRF3 signaling pathway. Nat. Immunol. *4*, 491–496.

Gohda, J., Matsumura, T., and Inoue, J. (2004). Cutting edge: TNFR-associated factor (TRAF) 6 is essential for MyD88-dependent pathway but not toll/IL-1 receptor domain-containing adaptor-inducing IFN-beta (TRIF)-dependent pathway in TLR signaling. J. Immunol. *173*, 2913–2917.

Hemmi, H., Takeuchi, O., Sato, S., Yamamoto, M., Kaisho, T., Sanjo, H., Kawai, T., Hoshino, K., Takeda, K., and Akira, S. (2004). The roles of two IkappaB kinase-related kinases in lipopolysaccharide and double stranded RNA signaling and viral infection. J. Exp. Med. *199*, 1641–1650.

Hiscott, J., Grandvaux, N., Sharma, S., Tenoever, B.R., Servant, M.J., and Lin, R. (2003). Convergence of the NF-kappaB and interferon signaling pathways in the regulation of antiviral defense and apoptosis. Ann. N Y Acad. Sci. *1010*, 237–248.

Hockenbery, D., Nunez, G., Milliman, C., Schreiber, R.D., and Korsmeyer, S.J. (1990). Bcl-2 is an inner mitochondrial membrane protein that blocks programmed cell death. Nature *348*, 334–336.

Honda, K., Yanai, H., Negishi, H., Asagiri, M., Sato, M., Mizutani, T., Shimada, N., Ohba, Y., Takaoka, A., Yoshida, N., and Taniguchi, T. (2005). IRF-7 is the master regulator of type-I interferon-dependent immune responses. Nature *434*, 772–777.

Inohara, N., del Peso, L., Koseki, T., Chen, S., and Nunez, G. (1998). RICK, a novel protein kinase containing a caspase recruitment domain, interacts with CLARP and regulates CD95-mediated apoptosis. J. Biol. Chem. *273*, 12296–12300.

Kang, D.C., Gopalkrishnan, R.V., Wu, Q., Jankowsky, E., Pyle, A.M., and Fisher, P.B. (2002). mda-5: an interferon-inducible putative RNA helicase with double-stranded RNA-dependent ATPase activity and melanoma growth-suppressive properties. Proc. Natl. Acad. Sci. USA *99*, 637–642.

Kato, H., Sato, S., Yoneyama, M., Yamamoto, M., Uematsu, S., Matsui, K., Tsujimura, T., Takeda, K., Fujita, T., Takeuchi, O., and Akira, S. (2005). Cell type-specific involvement of RIG-I in antiviral response. Immunity *23*, 19–28.

Kaufmann, T., Schlipf, S., Sanz, J., Neubert, K., Stein, R., and Borner, C. (2003). Characterization of the signal that directs Bcl-x(L), but not Bcl-2, to the mitochondrial outer membrane. J. Cell Biol. *160*, 53–64.

Kawai, T., Sato, S., Ishii, K.J., Coban, C., Hemmi, H., Yamamoto, M., Terai, K., Matsuda, M., Inoue, J., Uematsu, S., et al. (2004). Interferon-alpha induction through Toll-like receptors involves a direct interaction of IRF7 with MyD88 and TRAF6. Nat. Immunol. *5*, 1061–1068.

Kim, P.K., Hollerbach, C., Trimble, W.S., Leber, B., and Andrews, D.W. (1999). Identification of the endoplasmic reticulum targeting signal in vesicle-associated membrane proteins. J. Biol. Chem. *274*, 36876–36882.

Kovacsovics, M., Martinon, F., Micheau, O., Bodmer, J.L., Hofmann, K., and Tschopp, J. (2002). Overexpression of Helicard, a CARD-containing helicase cleaved during apoptosis, accelerates DNA degradation. Curr. Biol. *12*, 838–843.

Maniatis, T., Falvo, J.V., Kim, T.H., Kim, T.K., Lin, C.H., Parekh, B.S., and Wathelet, M.G. (1998). Structure and function of the interferon-beta enhanceosome. Cold Spring Harb. Symp. Quant. Biol. *63*, 609–620.

Matsuda, A., Suzuki, Y., Honda, G., Muramatsu, S., Matsuzaki, O., Nagano, Y., Doi, T., Shimotohno, K., Harada, T., Nishida, E., et al. (2003). Large-scale identification and characterization of human genes that activate NF-kappaB and MAPK signaling pathways. Oncogene *22*, 3307–3318.

McWhirter, S.M., Fitzgerald, K.A., Rosains, J., Rowe, D.C., Golenbock, D.T., and Maniatis, T. (2004). IFN-regulatory factor 3-dependent gene expression is defective in Tbk1-deficient mouse embryonic fibroblasts. Proc. Natl. Acad. Sci. USA *101*, 233–238.

Michaelson, D., Silletti, J., Murphy, G., D'Eustachio, P., Rush, M., and Philips, M.R. (2001). Differential localization of Rho GTPases in live cells: regulation by hypervariable regions and RhoGDI binding. J. Cell Biol. *152*, 111–126.

Perry, A.K., Chow, E.K., Goodnough, J.B., Yeh, W.C., and Cheng, G. (2004). Differential requirement for TANK-binding kinase-1 in type I interferon responses to toll-like receptor activation and viral infection. J. Exp. Med. *199*, 1651–1658.

Rehermann, B., and Nascimbeni, M. (2005). Immunology of hepatitis B virus and hepatitis C virus infection. Nat. Rev. Immunol. *5*, 215–229.

Schwer, B., Ren, S., Pietschmann, T., Kartenbeck, J., Kaehlcke, K., Bartenschlager, R., Yen, T.S., and Ott, M. (2004). Targeting of hepatitis C virus core protein to mitochondria through a novel C-terminal localization motif. J. Virol. *78*, 7958–7968.

Sharma, S., tenOever, B.R., Grandvaux, N., Zhou, G.P., Lin, R., and

Hiscott, J. (2003). Triggering the interferon antiviral response through an IKK-related pathway. Science *300*, 1148–1151.

Silverman, N., and Maniatis, T. (2001). NF-kappaB signaling pathways in mammalian and insect innate immunity. Genes Dev. *15*, 2321–2342.

Sumpter, R., Jr., Loo, Y.M., Foy, E., Li, K., Yoneyama, M., Fujita, T., Lemon, S.M., and Gale, M., Jr. (2005). Regulating intracellular antiviral defense and permissiveness to hepatitis C virus RNA replication through a cellular RNA helicase, RIG-I. J. Virol. *79*, 2689–2699.

Sun, L., and Chen, Z.J. (2004). The novel functions of ubiquitination in signaling. Curr. Opin. Cell Biol. *16*, 119–126.

tenOever, B.R., Sharma, S., Zou, W., Sun, Q., Grandvaux, N., Julkunen, I., Hemmi, H., Yamamoto, M., Akira, S., Yeh, W.C., et al. (2004). Activation of TBK1 and IKKvarepsilon kinases by vesicular stomatitis virus infection and the role of viral ribonucleoprotein in the development of interferon antiviral immunity. J. Virol. *78*, 10636–10649.

van Oers, N.S., and Chen, Z.J. (2005). Cell biology. Kinasing and clipping down the NF-kappa B trail. Science *308*, 65–66.

Wang, X. (2001). The expanding role of mitochondria in apoptosis. Genes Dev. *15*, 2922–2933.

Ye, H., Arron, J.R., Lamothe, B., Cirilli, M., Kobayashi, T., Shevde, N.K., Segal, D., Dzivenu, O.K., Vologodskaia, M., Yim, M., et al. (2002). Distinct molecular mechanism for initiating TRAF6 signalling. Nature *418*, 443–447.

Yoneyama, M., Suhara, W., and Fujita, T. (2002). Control of IRF-3 activation by phosphorylation. J. Interferon Cytokine Res. *22*, 73–76.

Yoneyama, M., Kikuchi, M., Natsukawa, T., Shinobu, N., Imaizumi, T., Miyagishi, M., Taira, K., Akira, S., and Fujita, T. (2004). The RNA helicase RIG-I has an essential function in double-stranded RNA-induced innate antiviral responses. Nat. Immunol. *5*, 730–737.

Accession Numbers

The GenBank accession number for the human *MAVS* is DQ174270 and for the mouse *MAVS* is DQ174271.